Analytical Reformulation of Chance-Constrained Optimal Power Flow with Uncertain Load Control

Bowen Li and Johanna L. Mathieu
EECS, University of Michigan, USA
{libowen, jlmath}@umich.edu

***Abstract*—Aggregations of controllable loads can provide reserves to power systems; however, their reserve capacity is uncertain and affected by ambient conditions like weather. Past work proposed a stochastic optimal power flow formulation that used chance constraints to handle uncertain reserves and generation from wind. The problem was solved with a scenario-based optimization method. In this paper, we assume Gaussian distributions of all uncertainties and reformulate the constraints analytically to solve a deterministic problem, which is computationally simpler than scenario-based approaches. To evaluate this idea, we implement our method on a modified IEEE 30-bus network and compare our results to those of a scenario-based method. Use of low-cost but uncertain load reserves yields lower cost dispatch solutions than those for systems with only generator reserves. The analytical approach using a cutting plane algorithm leads to fast convergence and is scalable to larger problem sizes. We explore the effect of non-Gaussian and correlated uncertainties on the reliability of the solution.**

***Index Terms*—load control, optimal power flow, stochastic optimization**

I. Introduction

Aggregations of controllable loads can provide reserves to power systems, possibly with faster response and lower price than conventional resources [1]. Unlike generator reserves, load reserves are uncertain and time varying because load usage patterns and ambient conditions affect load flexibility [2]. In previous research, an aggregated thermal energy storage model was used to estimate the reserve capacity of an aggregation of thermostatically controlled loads as a function of outdoor temperature [3]. Using this model, a stochastic optimal power flow (OPF) was proposed to handle wind and temperature uncertainty and solve for a day-ahead hourly generation and reserve schedule [4]. The problem was formulated as a chance-constrained OPF problem and solved with probabilistically robust design [6], inspired by the so-called scenario approach [5]. The scenario approach transforms probability constraints into hard constraints corresponding to a specific number of uncertainty scenarios. By using a sufficient number of scenarios, and without knowing the exact uncertainty distributions, the approach ensures a-priori guarantees that the optimal solution will satisfy the probability constraints with a certain level of confidence [5]. With high problem dimension, the computational time and memory usage is large, and the approach in [6] mitigates these issues by reformulating the problem into a robust optimization problem.

In contrast, analytical reformulation is an inverse operation that transforms probability constraints into deterministic constraints using knowledge of uncertainty distributions. For the case in which all errors are Gaussian with mutual independence, [7] gives a reformulation for the regular OPF problem and [8] for the security constrained OPF problem. The benefit of analytical reformulation is low computational complexity with comparable (or better) objective costs and reliability as compared to scenario-based methods (assuming the true uncertainty distributions are equivalent to the assumed ones). A convexity check on the new formulation is required to ensure global optimality. Past work has not applied this method to OPF problems with uncertain reserves.

In this paper, we analytically reformulate the stochastic OPF presented in [4] under the assumption of Gaussian and uncorrelated wind and temperature uncertainty. We explore the performance and computational complexity of this approach as compared to scenario-based methods in both uncongested and congested cases, using a modified IEEE 30-bus system. Additionally, we use an iterative solving algorithm from [7], which helps accelerate convergence, and check the reliability of our solution using empirical scenarios, correlated Gaussian errors, and non-Gaussian errors.

II. Load model

We model aggregations of thermal loads such as air conditioners as thermal energy storage devices [3]. We assume a load aggregator sends on/off control signals to the loads in order to change their aggregate power consumption $P_{C,t}$, but that all stay within a narrow ($\sim 1^{\circ}$C) temperature range around their set point temperature. The difference between $P_{C,t}$ and the baseline power consumption $P_T(T_t)$ linearly affects the aggregation's energy state S_t

$$S_{t+\Delta\tau}(T_t) = S_t + (P_{C,t} - P_T(T_t))\Delta\tau \tag{1}$$

where t is the time index, $\Delta\tau$ is the time step. $P_{C,t}$ and S_t are bounded but their capacities are functions of ambient temperature T_t. Ref. [3] describes a method to compute these capacities. Within our analytical reformulation, we model them as piece-wise linear functions of temperature (using two lines), which is a good approximation given Fig. 1 of [4]. We assume the baseline power is linear in temperature.

III. Problem formulation

Our day-ahead, 24-hour, stochastic OPF problem is similar to that of [4]. In this section, we summarize the problem and highlight the differences in our formulation. Our goal is to minimize energy and reserve costs

$$\min_{\{x_t\}_{t=1}^{24}} \sum_{t=1}^{24} (x_t^T[c_1]x_t + c_2^T x_t) \tag{2}$$

This work was supported by NSF Grant #CCF-1442495.

subject to deterministic and probabilistic constraints, detailed in the following subsections. Parameters c_1 and c_2 include the first and second order generation and reserve costs. Assume we have N_G generators, N_L controllable loads, N_W wind power plants, and N_B buses. The design variable vector x_t includes generation $P_{G,t} \in \mathbb{R}^{N_G}$, controllable loads set points $P_{C,t} \in \mathbb{R}^{N_L}$, generator reserve capacities $R_{GS,t}^{up/dn}$, $R_{GD,t}^{up/dn,k} \in \mathbb{R}^{N_G}$ (where S refers to secondary control and D refers to re-dispatch; and up/dn refer to the up/down reserve limits; and there are four types k of re-dispatch, described in the following subsections), and load reserve capacities $R_{LS,t}^{up/dn} \in \mathbb{R}^{N_L}$. It also includes "distribution vectors" $d_{GS,t}$, $d_{GD,t}^{k} \in \mathbb{R}^{N_G}$ and $d_{LS,t} \in \mathbb{R}^{N_L}$ that distribute the real time power mismatch to reserve-providing resources [9]. To simplify our analysis, we do not allow for different distribution vectors for up and down reserves as [4] does. All design variables are constrained to be greater than or equal to zero.

A. Uncertainty Notation

Let $\mu_{w,t,i}$ and $\delta_{w,t,i}$ denote the mean and standard deviation of the output of the i-th wind power plant, and $\mu_{w,t}$ and $\delta_{w,t}$ the mean and standard deviation of the total wind power mismatch $P_{m,t}$. Denote the i-th wind power plant's forecast error as $\Delta_{w,t,i}$ and error vector containing all forecast errors as $\Delta_{w,t}$. Define the notation for baseline power error similarly: $\mu_{P,t,i}$ and $\delta_{P,t,i}$ denote the mean and standard deviation of the baseline power of the i-th load; $\mu_{P,t}$ and $\delta_{P,t}$ the mean and standard deviation of total baseline power error $P_{m,t}^{b}$; $\Delta_{P,t,i}$ the i-th loads' baseline power forecast error; and $\Delta_{P,t}$ the error vector. In this paper, for simplicity, we assume all loads experience the same temperature (though this is not a requirement of our approach) and so use $\mu_{T,t}$, $\delta_{T,t}$, and $\Delta_{T,t}$ to denote the mean, standard deviation, and forecast error of the temperature. Since the baseline error is linearly related to temperature error, $\Delta_{P,t} = a\Delta_{T,t}$ where a is a constant.

B. Deterministic Constraints

The following power and energy constraints are deterministic, using forecasted values (denoted with superscript f) to determine the generation schedule [4]:

$$\mathbf{1}_{1\times N_B} P_{inj,t} = 0 \tag{3}$$
$$-P_l \le AP_{inj,t} \le P_l \tag{4}$$
$$\underline{P}_G \le P_{G,t} \le \overline{P}_G \tag{5}$$
$$\underline{0} \le P_{C,t} \le \overline{P}_C(T_t^f) \tag{6}$$
$$0 \le S_t \le \overline{S}(T_t^f) \tag{7}$$
$$0 \le S_{t+\Delta\tau}(T_t^f) \le \overline{S}(T_t^f) \tag{8}$$

where $P_{inj,t} = \Big(C_G P_{G,t} + C_W P_{w,t}^f - C_L(P_{L,t} + P_{C,t})\Big)$. Equation (3) is the power balance where C_G, C_W, C_L are matrices mapping generators/load to their corresponding buses and $P_{L,t} \in \mathbb{R}^{N_L}$ is the uncontrollable load. Equations (4)-(8) bound the power flow, generation, load set points, and energy state (at the beginning an end of each interval), where P_l contains the transmission line limits and A is a constant matrix that transforms power injections into power flow [9].

C. Probabilistic Constraints

All constraints that include uncertainty are formulated as individual chance constraints, for example, $\Pr(a_t x_{i,t} \le b_t) \ge 1-\epsilon$ where a_t, b_t are uncertain and ϵ is the chance of constraint violation. We assume that both loads and generators can provide secondary control to balance real-time deviations from forecasts, and that generators are re-dispatched every 15 minutes. We define four types of re-dispatch associated with compensating 0) energy mismatch from the previous hour, 1) intra-hour wind power mismatch, 2) intra-hour energy mismatch, and 3) baseline power mismatch. Ref. [4] considered 0-2 but neglected 3, which increases the problem dimension but enables better tracking of the load energy states.

1) Secondary Frequency Control: The secondary control power constraints are

$$-P_l \le AP_{injSec,t} \le P_l \tag{9}$$
$$\underline{P}_G \le P_{G,t} - d_{GS,t}P_{m,t} + d_{GD,t}^3 P_{m,t}^b \le \overline{P}_G \tag{10}$$
$$0 \le P_{C,t} + d_{LS,t}P_{m,t} + \Delta_{P,t} \le \overline{P}_C(T_t) \tag{11}$$
$$-R_{GS,t}^{dn} \le -d_{GS,t}P_{m,t} \le R_{GS,t}^{up} \tag{12}$$
$$-R_{LS,t}^{dn} \le d_{LS,t}P_{m,t} \le R_{LS,t}^{up} \tag{13}$$
$$-R_{GD,t}^{dn,3} \le d_{GD,t}^3 P_{m,t}^b \le R_{GD,t}^{up,3} \tag{14}$$
$$\mathbf{1}_{1\times N_G} d_{GS,t} + \mathbf{1}_{1\times N_L} d_{LS,t} = 1 \tag{15}$$
$$\mathbf{1}_{1\times N_G} d_{GD,t}^3 = 1 \tag{16}$$

where $P_{injSec,t} = C_G(P_{G,t} - d_{GS,t}P_{m,t} + d_{GD,t}^3 P_{m,t}^b) + C_w P_{w,t} - C_L(P_{L,t} + P_{C,t} + d_{LS,t}P_{m,t} + \Delta_{P,t})$. Equations (9)-(11) are similar to (4)-(6) but include deviations due to secondary reserve provision and baseline power error (which is compensated for by the generators). The deviations are bounded by reserve capacities in (12)-(14). Equations (15) and (16) ensure the total deviation matches the total error.

Provision of secondary control causes the energy states of the loads to deviate from their forecast trajectories. We need to ensure that each load's energy state stays within its energy limits. Fortunately, since the energy dynamics are linear, we only need to check the start/end points of each 15 minute interval. To simplify notation, we denote the forecast energy trajectory S_t^f and forecast baseline power $P_{T,t}^f$. The energy constraints are

$$0 \le S_t^f + \underbrace{\Big(P_{C,t} + d_{LS,t}P_{m,t} - P_{T,t}^f - \Delta_{P_T,t}\Big)}_{P_{D,t}} \frac{\Delta\tau}{4} \le \overline{S}(T_t) \tag{17}$$
$$0 \le S_t^f + \frac{\Delta\tau}{4}\Delta_{P_T,t-1} \le \overline{S}(T_t) \tag{18}$$
$$0 \le S_t^f + \Big(P_{C,t} - P_{T,t}^f\Big)\frac{3\Delta\tau}{4} + P_{D,t}\frac{\Delta\tau}{4} \le \overline{S}(T_t) \tag{19}$$
$$0 \le S_t^f + \Big(P_{C,t} - P_{T,t}^f\Big)\frac{3\Delta\tau}{4} + \Delta_{P_T,t}\frac{\Delta\tau}{4} \le \overline{S}(T_t) \tag{20}$$
$$0 \le S_t^f + \Big(P_{C,t} - P_{T,t}^f\Big)\frac{3\Delta\tau}{4} + P_{D,t}\frac{\Delta\tau}{4} \le \overline{S}(T_{t+1}) \tag{21}$$

where (17) and (18) bound actions in the first 15 minutes, and (19) and (20) in the last 15 minutes. Equation (21) checks the energy constraints in the next hour.

2) Re-dispatch: The re-dispatch constraints are similar to secondary control constraints except $d_{GS,t}$ is replaced by $d^1_{GD,t} + d^2_{GD,t}$ in (9) and (10), the sign of $d_{LS,t}$ is reversed in (9) and (11), and the following constraints are added

$$-R^{dn}_{GD,t} \leq -(d^1_{GD,t} + d^2_{GD,t})P_{m,t} \leq R^{up}_{GD,t} \tag{22}$$

$$\mathbf{1}_{1\times N_G} d^1_{GD,t} = 1, \tag{23}$$

$$\mathbf{1}_{1\times N_G} d^2_{GD,t} = \mathbf{1}_{1\times N_L} d_{LS,t}, \tag{24}$$

where $R^{dn}_{GD,t} = R^{dn,1}_{GD,t} + R^{dn,2}_{GD,t}$ and $R^{up}_{GD,t} = R^{up,1}_{GD,t} + R^{up,2}_{GD,t}$.

As in [4], we also use coupling constraints that allow us to handle energy mismatch from the previous hour, in the first 15 minutes of the current hour. We must consider two cases: i) both re-dispatch and secondary control are active during these first 15 minutes and ii) only re-dispatch is active. For i), we replace $d_{GS,t}P_{m,t}$ with $d_{GS,t}P_{m,t} + d^0_{GD,t}P_{m,t-1}$ in (9) and (10) and $d_{LS,t}P_{m,t}$ with $-d_{LS,t-1}P_{m,t-1} + d_{LS,t}P_{m,t}$ in (11) and (13). For ii), we replace $d_{GS,t}P_{m,t}$ with $d^0_{GD,t}P_{m,t-1}$ and $d_{LS,t}P_{m,t}$ with $-d_{LS,t-1}P_{m,t-1}$. Additional constraints include:

$$-R^{dn,0}_{GD,t} \leq -d^0_{GD,t}P_{m,t-1} \leq R^{up,0}_{GD,t} \tag{25}$$

$$\mathbf{1}_{1\times N_G} d^0_{GD,t} = \mathbf{1}_{1\times N_L} d_{LS,t-1}, \tag{26}$$

$$0 \leq S^f_t + (P_{C,t} + d_{LS,t}P_{m,t} - d_{LS,t-1}P_{m,t-1} - P^f_{T,t} - \Delta_{P,t})\frac{\Delta\tau}{4} \leq \overline{S}(T_t) \tag{27}$$

IV. Analytical reformulation

The biggest challenges in analytically reformulating the problem are the complexity of the constraints and large number of uncertain variables. Though we assume Gaussian temperature forecast error, the load power/energy capacities are modeled as piecewise linear functions of temperature and so the power/energy capacity error is non-Gaussian.

A. Secondary Frequency Control Constraint Reformulation

Constraints with only one uncertain variable are reformulated into linear constraints and constraints with two uncertain variables are reformulated into 2-norms since we assume uncertainties are independent Gaussian random variables. As each inequality constraint is bounded on two sides, each results in two equations. The constant c is a scalar computed as $\Phi^{-1}(1-\epsilon)$, where Φ is the cumulative density function (CDF) of the relevant random variable. Let $\mathbb{S}_*$ denote slack variables. The power constraints can be reformulated as

$$P_G - d_{GS,t}\mu_{w,t} + d^3_{GD,t}\mu_{P,t} + \mathbb{S}_{GS,t} \leq \overline{P}_G \tag{28}$$

$$P_G - d_{GS,t}\mu_{w,t} + d^3_{GD,t}\mu_{P,t} - \mathbb{S}_{GS,t} \geq \underline{P}_G \tag{29}$$

$$\mathbb{S}_{GS,t} \geq c\sqrt{(d_{GS,t}\delta_{w,t})^2 + (d^3_{GD,t}\delta_{P,t})^2} \tag{30}$$

$$P_C + g_1 \leq \overline{P}_C(T^f_t) \tag{31}$$

$$P_C + d_{LS,t}\mu_{w,t} + a\mu_{T,t} - \mathbb{S}_{LS,t} \geq 0 \tag{32}$$

$$\mathbb{S}_{LS,t} \geq c\sqrt{(d_{LS,t}\delta_{w,t})^2 + (a\delta_{T,t})^2} \tag{33}$$

$$R^{up}_{GS,t} \geq -d_{GS,t}\mu_{w,t} + cd_{GS,t}\delta_{w,t} \tag{34}$$

$$R^{dn}_{GS,t} \geq d_{GS,t}\mu_{w,t} + cd_{GS,t}\delta_{w,t} \tag{35}$$

$$R^{up}_{LS,t} \geq d_{LS,t}\mu_{w,t} + cd_{LS,t}\delta_{w,t} \tag{36}$$

$$R^{dn}_{LS,t} \geq -d_{LS,t}\mu_{w,t} + cd_{LS,t}\delta_{w,t} \tag{37}$$

$$R^{up,3}_{GD,t} \geq d^3_{GD,t}\mu_{P,t} + cd^3_{GD,t}\delta_{P,t} \tag{38}$$

$$R^{dn,3}_{GD,t} \geq -d^3_{GD,t}\mu_{P,t} + cd^3_{GS,t}\delta_{P,t} \tag{39}$$

where (28)-(33) are the reformulation of (10) and (11), and g_1 is function describing the intersection of five supporting planes providing a convex approximation of the nonlinear confidence level bound related to the load power capacity (more details given in Section IV-E). Reserve capacity constraints (12)-(14) are reformulated as (34)-(39).

The upper bounds of the energy constraints (17)-(21) are reformulated as

$$S^f_t + (P_{C,t} - P^f_{T,t})\frac{\Delta\tau}{4} + g_3 \leq \overline{S}(T^f_t) \tag{40}$$

$$S^f_t + g_2 \leq \overline{S}(T^f_t) \tag{41}$$

$$S^f_t + P_{C,t} - P^f_{T,t} + g_3 \leq \overline{S}(T^f_t) \tag{42}$$

$$S^f_t + (P_{C,t} - P^f_{T,t})\frac{3\Delta\tau}{4} + g_2 \leq \overline{S}(T^f_t) \tag{43}$$

$$S^f_t + P_{C,t} - P^f_{T,t} + g_4 \leq \overline{S}(T^f_{t+1}) \tag{44}$$

where all g_i, like g_1, are piece-wise linear convex approximations. The lower bounds of the energy constraints require a slack variable $\mathbb{S}_{EC,t}$

$$S^f_t + (P_{C,t} - P^f_{T,t} + d_{LS,t}\mu_{w,t} - a\mu_{T,t})\frac{\Delta\tau}{4} - \mathbb{S}_{EC,t} \geq 0 \tag{45}$$

$$S^f_t + (\mu_{P,t-1} - ac\delta_{T,t-1})\frac{\Delta\tau}{4} \geq 0 \tag{46}$$

$$S^f_t + P_{C,t} - P^f_{T,t} + (d_{LS,t}\mu_{w,t} - a\mu_{T,t})\frac{\Delta\tau}{4} - \mathbb{S}_{EC,t} \geq 0 \tag{47}$$

$$S^f_t + (P_{C,t} - P^f_{T,t})\frac{3\Delta\tau}{4} + (\mu_{P,t} - ac\delta_{T,t})\frac{\Delta\tau}{4} \geq 0 \tag{48}$$

$$\mathbb{S}_{EC,t} \geq \frac{c\Delta\tau}{4}\sqrt{(d_{LS,t}\delta_{w,t})^2 + (a\delta_{T,t})^2} \tag{49}$$

B. Re-dispatch Constraint Reformulation

The reformulated re-dispatch power constraints are similar to the reformulated secondary control power constraints. We simply define $d_{GD,t} = d^1_{GD,t} + d^2_{GD,t}$, replace $d_{GS,t}$ with $d_{GD,t}$, reverse the sign of $d_{LS,t}$, and change the design/slack variables in (28)-(39).

Reformulating the coupling constraints again requires consideration of two cases. When secondary control is not active, we can simply replace $d_{GS,t}$ with $d^0_{GD,t}$, $d_{LS,t}$ with $-d_{LS,t-1}$, and use $P_{m,t-1}$ instead of $P_{m,t}$. When secondary control is active, we need the following constraints

$$d_{LS,t}\mu_{w,t} - d_{LS,t-1}\mu_{w,t-1} + \mathbb{S}^1_{CP,t} \leq R^{up}_{LS,t} \tag{50}$$

$$d_{LS,t}\mu_{w,t} - d_{LS,t-1}\mu_{w,t-1} - \mathbb{S}^1_{CP,t} \geq -R^{dn}_{LS,t} \tag{51}$$

$$\mathbb{S}^1_{CP,t} \geq c\sqrt{(d_{LS,t}\delta_{w,t})^2 + (d_{LS,t-1}\delta_{w,t-1})^2} \tag{52}$$

$$P_G - d_{GS,t}\mu_{w,t} - d^0_{GD,t}\mu_{w,t-1} + d^3_{GD,t}\mu_{P,t} + \mathbb{S}^2_{CP,t} \leq \overline{P}_G \tag{53}$$

$$P_G - d_{GS,t}\mu_{w,t} - d^0_{GD,t}\mu_{w,t-1} + d^3_{GD,t}\mu_{P,t} - \mathbb{S}^2_{CP,t} \geq \underline{P}_G \tag{54}$$

$$\mathbb{S}^2_{CP,t} \geq c\sqrt{(d_{GS,t}\delta_{w,t})^2 + (d^0_{GD,t}\delta_{w,t-1})^2 + (d^3_{GD,t}\delta_{P,t})^2} \tag{55}$$

$$P_C + g_5 \leq \overline{P}_C(T^f_t) \tag{56}$$

$$P_C+d_{LS,t}\mu_{w,t}-d_{LS,t-1}\mu_{w,t-1}+a\mu_{T,t}-S^3_{CP,t}\geq 0 \quad (57)$$

$$\mathbb{S}^3_{CP,t}\geq c\sqrt{(d_{LS,t}\delta_{w,t})^2+(d_{LS,t-1}\delta_{w,t-1})^2+(a\delta_{T,t})^2} \quad (58)$$

$$S^f_t+\frac{\Delta\tau}{4}(P_{C,t}-P^f_{T,t})+g_6\leq\overline{S}(T^f_t) \quad (59)$$

$$S^f_t+\frac{\Delta\tau}{4}(P_{C,t}-P^f_{T,t}+d_{LS,t}\mu_{w,t}-d_{LS,t}\mu_{w,t-1}-a\mu_{T,t} -\mathbb{S}^3_{CP,t})\geq 0 \quad (60)$$

where g_i are again convex approximations.

C. Power Flow Constraint Reformulation

The analytical reformulation for power flow constraints is more complex than the previous reformulations. All uncertainties appear in $P_{inj,t}$ and design variables related to reserve provision can exist in the constraints. We use the secondary control power flow constraint (9) as an example. Denote the power flow from bus i to j as f_{ij} with β_{ij} the admittance between those 2 buses. Then,

$$f_{ij}=\beta_{ij}(\theta_i-\theta_j) \quad (61)$$

where $\theta_i=(\breve{B}P_{inj,t})_i$, $\theta_j=(\breve{B}P_{inj,t})_j$, and $\breve{B}$ is a constant matrix related to admittance matrix with the same definition as in [7]. Separate the power injection equation into three parts: forecast, secondary control, and re-dispatch

$$P^f_{inj,t}=C_GP_{G,t}+C_wP^f_{w,t}-C_L(P_{L,t}+P_{C,t}) \quad (62)$$

$$P^{sc}_{inj,t}=C_GR_{GS,t}+C_w\Delta_{w,t}-C_LR_{LS,t} \quad (63)$$

$$P^{rd}_{inj,t}=C_GR^3_{GD,t}-C_L\Delta_{P,t} \quad (64)$$

$$\theta_i=\left(\breve{B}(P^f_{inj,t}+P^{sc}_{inj,t}+P^{rd}_{inj,t})\right)_i \quad (65)$$

Define the following matrices:

$$G=[\breve{B}C_G]_{N_B\times N_G} \qquad B=[\breve{B}C_W]_{N_B\times N_W}$$
$$C=[\breve{B}C_L]_{N_B\times N_L} \qquad D=[\breve{B}C_Gd_{GS,t}]_{N_B\times 1}$$
$$E=[\breve{B}C_Ld_{LS,t}]_{N_B\times 1} \qquad F=[\breve{B}C_Gd^3_{GD,t}]_{N_B\times 1}$$

Then, we have

$$f^{sc}_{ij}=\beta_{ij}((B\Delta_{w,t})_i-(D+E)_ie^T\Delta_{w,t} -(B\Delta_{w,t})_j+(D+E)_je^T\Delta_{w,t}) \quad (66)$$

$$f^{rd}_{ij}=\beta_{ij}(F_ie^T\Delta_{P,t}-(C\Delta_{P,t})_i -F_je^T\Delta_{P,t}+(C\Delta_{P,t})_j) \quad (67)$$

We can now write the full reformulation of the power flow constraint as a function of the baseline power and wind forecast error at each each bus at each bus k

$$c_k=[B_{ik}-B_{jk}-(D+E)_i+(D+E)_j] \quad (68)$$

$$d_k=(F_i-F_j-C_{ik}+C_{jk})a_k \quad (69)$$

$$\mu^{sc}_{ij}=\beta_{ij}\sum_{k=1}^{N_W}c_k\mu_{w,t,k} \quad (70)$$

$$\mu^{rd}_{ij}=\beta_{ij}\left(\sum_{k=1}^{N_L}d_k\right)\mu_{T,t} \quad (71)$$

$$p_{ij}=\beta_{ij}((G_i-G_j)P_{G,t}+(B_i-B_j)P^f_{w,t} -(C_i-C_j)(P_{L,t}+P_{C,t})) \quad (72)$$

$$p_{ij}+\mu^{sc}_{ij}+\mu^{rd}_{ij}+\mathbb{S}_{ij}\leq P_l \quad (73)$$

$$p_{ij}+\mu^{sc}_{ij}+\mu^{rd}_{ij}-\mathbb{S}_{ij}\geq -P_l \quad (74)$$

$$\mathbb{S}_{ij}\geq c\left\|\beta_{ij}\left[c_1\delta_{w,t,1},\ldots,c_{N_W}\delta_{w,t,N_W},\left(\sum_{k=1}^{N_L}d_k\right)\delta_{T,t}\right]\right\|_2 \quad (75)$$

where G_i as the i-th row of G and $\Delta_{P,t,k}=a_k\Delta_{T,t}$.

D. Cutting Plane Algorithm

To reduce computational complexity, we have replaced some complicated constraints with slack variables. We apply the iterative cutting plane method described in [7]. Consider (28) in which we use $\mathbb{S}_{GS,t}$ instead of the nonlinear constraint (30). Assume we obtain optimal decision variables for the problem without (30). We evaluate (30) and if it is satisfied, we have a solution to the full problem. If not, we introduce a new constraint

$$\mathbb{S}_{GS,t}\geq f(\cdot)+\frac{\partial f(\cdot)}{\partial d_{GS,t}}\Delta(R^{up}_{GS,t})+\frac{\partial f(\cdot)}{\partial d^3_{GD,t}}\Delta(d^3_{GD,t}) \quad (76)$$

where $f(\cdot)$ is the right side of (30), and resolve the problem. In a finite number of iterations, we get a result which satisfies all of the constraints. To further reduce the iteration time, we include the following constraints, which comprise a relaxation with a feasible region 27% larger than the cone space.

$$\mathbb{S}_{GS,t}\geq cd_{GS,t}\delta_{w,t}$$
$$\mathbb{S}_{GS,t}\geq cd^3_{GD,t}\delta_{P,t}$$
$$\mathbb{S}_{GS,t}\geq\frac{c\sqrt{2}}{2}(d_{GS,t}\delta_{w,t}+d^3_{GD,t}\delta_{P,t})$$

This technique is also used for power flow and some energy capacity constraints.

E. Probability Analysis and Convex Approximation

We use many convex approximations g_i, which are required because load power/energy capacity forecast errors are non-Gaussian. Take the secondary control power capacity constraint (31) as an example. To find the function g_1, we need to solve for the confidence bound for

$$\mathrm{P}(d_{LS,t}P_{m,t}+\Delta_{P,t}-e_{\overline{P}_C(\Delta_{T,t})}\leq g_1)\geq 99\% \quad (77)$$

where $e_{\overline{P}_C(\Delta_{T,t})}$ is the power capacity error, which is a piecewise linear function of $\Delta_{T,t}$. Function g_1 is also a function of $d_{LS,t}$. To simplify the derivation, we rewrite the quantity within probability operator as $Z=\max(k_1x,k_2x+h)+dy=M+dy$ where x is $\Delta_{T,t}$; y is $P_{m,t}$; $k_1<0$, $k_2>0$, and $h<0$ are constants; M is lower bounded by constant C_1; and d is $d_{LS,t}$, which is a design variable. Let the CDF and probability density function (PDF) of $x=\Delta_{T,t}$ be $F_X(x)$ and $f_x(x)$. Now we can find the CDF for M

$$\Pr(M\leq m)=F_X\left(\frac{m-h}{k_2}\right)-F_X\left(\frac{m}{k_1}\right) \quad (78)$$

and the PDF for M

$$f_m(m)=\frac{d\mathrm{P}(M\leq m)}{dm}=\frac{f_x(\frac{m-h}{k_2})}{k_2}-\frac{f_x(\frac{m}{k_1})}{k_1} \quad (79)$$

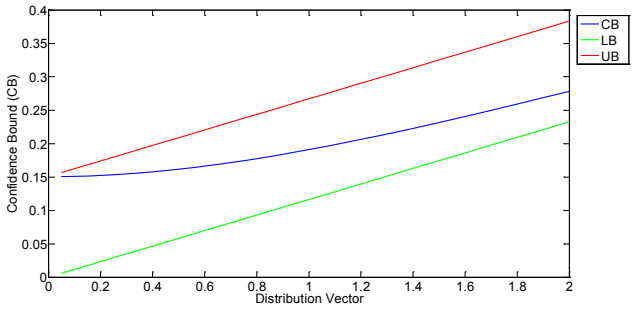

Fig. 1. The 99% confidence bound associated with the secondary control power capacity constraint.

Let the PDF and CDF of $N = dy$ be $f_{N,d}(n)$ and $\Phi_{N,d}(n)$. Now we can find the CDF for Z

$$\mathrm{P}(Z \leq g_1(d)) = \int_{C_1}^{\infty} f_m(m)\Phi_{N,d}(g_1(d) - m)dm \geq 99\% \quad (80)$$

For other g_i, the methodology will be the same with different constant values. As there is no symbolic equation for g_i and $d \in [0, 1]$, we use visual inspection to check the convexity and other properties. In Fig. 1, we see that the confidence bound shows convexity and that the function is non-decreasing on $d > 0$. To use this bound in our simulation, we construct a supporting plane set $g_1 \geq \max(p_{1,j}d_{LS,t} + q_{1,j})$ for $j = 1, \ldots, 5$, where $p_{1,j}$ and $q_{1,j}$ are the slopes and intercepts. This convex approximation gives us a close estimate of the original set and only introduces linear constraints into the optimization.

V. Simulation Setup

We solved the problem for a modified IEEE 30-bus system with single wind power generator on bus 13. All loads were assumed 50% controllable and the uncontrollable portion was scaled with a shifted sine wave with peaks (set equal to values in the test case [10]) at $t = 18$. We use the same look-up table relating power/energy capacities of 1000 heat pump heaters to outdoor temperature as in [4], and assume time varying temperature forecast (shifted sine wave with peak of 12°C at $t = 16$). We considered both uncongested and congested power flow by reducing the transmission line limits between bus 1 and bus 2 from 160 MVA to 110 MVA. For each case, we used both the scenario-based method developed in [6] (and applied in [4]) and analytical reformulation with $\epsilon = 99\%$.

We use the same wind and temperature error scenarios as in [4], but we use time-varying wind forecasts (following a cosine function with a peak of 55MW and no phase shift) to normalize the wind error. The distributions of both types of errors are approximately Gaussian. We assume load reserves are cheaper than generator reserves but the costs are still comparable. Load reserves on different buses were assigned different costs: $[5.7, 5.3, 5.1, 5, 5.1, 5.3, 5.7, 6.3, 6.9, 7.5, 8.1, 8.8, 9.3, 9.7, 9.9, 10, 9.9, 9.7, 9.3, 8.8, 8.2]$ \$/MW. Generation costs were set to the values from the test case [10], secondary control costs were set to the first order generation costs with scale factor of 1.5, and re-dispatch costs were set to the first order generation costs. All optimization problems were solved by CVX with Mosek and Gurobi.

VI. Simulation Results

Figures 2 and 5 show the scheduled reserve capacity of several generators and loads in the uncongested and congested case, respectively. In the uncongested case, the system prioritizes low cost reserves (load bus 5), while in the congested case the transmission constraint between bus 1 and 2 prevents some of load bus 5's reserves from being utilized. Fewer reserves are procured when the problem is solved analytically (a) because the scenario-based approach (s) is heavily influenced by outliers and so gives more conservative results. Additionally, the analytical formulation produces a smoother curve. Figures 3 and 6 show the generation schedule of several of the generators in the uncongested and congested case, respectively. In the uncongested case, analytical reformulation works better to shift load and mitigate the generation peak at $t = 16$. This is because the scenario-based method treats uncertainties more conservatively, leaving less room for peak shifting. In the congested cases, the results for generator 1 are more similar between the two approaches, but the scenario-based method calls on generator 5, which is more expensive, to alleviate the peak. Figures 4 and 7 show the set point of several of the controllable loads in the uncongested and congested case, respectively. The set points produced by the analytical approach deviate more than those produced by the scenario-based method because the analytical approach is less conservative. The reason why the set point rises at beginning is to pre-charge the thermal storage so that the load can drop below baseline during the peak loading period $t = 12, \ldots, 18$.

Table I shows the computation time associated with two approaches. We solved the analytical reformation with both a nonlinear solver and with the cutting-plane algorithm. For the uncongested case, the slack variables are unlikely to be active and the cutting-plane method is fast. For the congested case, the cutting plane method is slower. The computational effort of the scenario approach is less sensitive to congestion. Although here, cutting-plane methods are comparable with scenario-based methods in terms of computational time, with more uncertain variables, the number of constraints in scenario-based method will increase exponentially, while the size of the analytically-reformulated problem will remain the same. Table II shows the breakdown in costs while Table III shows the reliability results. We prepared three sets of data – the empirical scenarios, randomly generated correlated Gaussian errors, and randomly generated Weibull distributed errors – and performed 4000 Monte Carlo runs to test the probability of joint and individual constraint violations. In the uncongested case, the scenario-based method is resilient to all errors due to its conservativeness. As expected, the analytical approach provides less joint reliability, especially under the Weibull distribution. The individual reliability is still comparable with our requirement. For the congested case, there is slight decrease in all reliability levels due to a higher risk of violating transmission line constraints.

VII. Conclusions

In this paper, we presented the full analytical formulation for the stochastic optimal power flow problem with uncertain load control and uncertain wind production under the assumption of Gaussian outdoor temperature and wind uncertainty. We

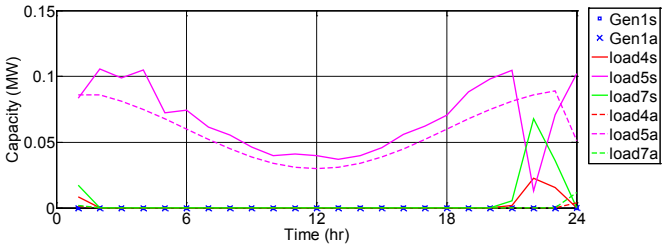

Fig. 2. Reserve capacity, uncongested.

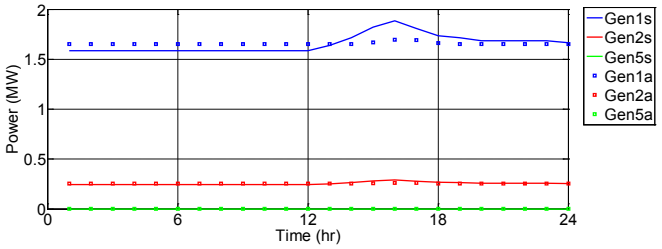

Fig. 3. Generator schedules, uncongested.

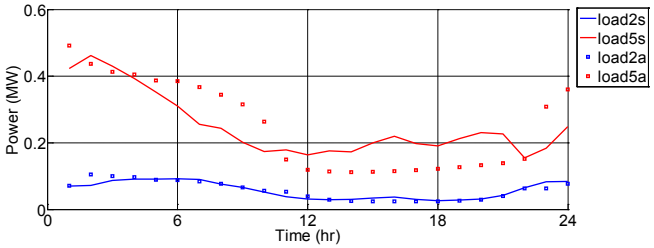

Fig. 4. Load schedules, uncongested.

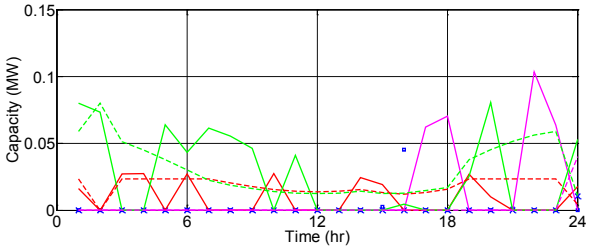

Fig. 5. Reserve capacity, congested.

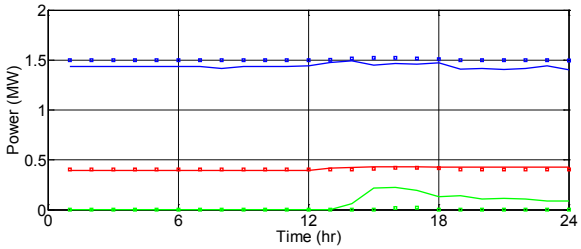

Fig. 6. Generator schedules, congested.

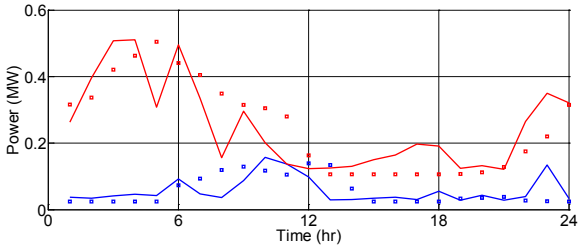

Fig. 7. Load schedules, congested.

TABLE I
COMPUTATIONAL TIME

	Scenario	Analytical	
		Nonlinear	Cutting
uncongested	11.57	12.79	5.94
congested	12.32	42.34	15.21

compared the performance and computational complexity of this approach to that of a scenario-based methods. We found that the analytical approach provides less conservative results with better objective values and more effective response to peak load and congestion. The scenario-based method provides high joint and individual constraint satisfaction, while with analytical reformulation, joint reliability suffers.

TABLE II
COST DISTRIBUTION

		Scenario	Analytical
uncongested	generation	121010	120850
	secondary	1821	1443
	redispatch	52696	42127
congested	generation	123960	122460
	secondary	2134	1529
	redispatch	52487	42085

TABLE III
RELIABILITY RESULTS (UNCONGESTED/CONGESTED)

		Scenario	Analytical
empirical scenarios	Joint	0.996/0.994	0.890/0.854
	Individual	0.999/0.998	0.976/0.967
correlated errors	Joint	0.994/0.994	0.892/0.869
	Individual	0.998/0.998	0.980/0.974
Weibull distributed errors	Joint	0.995/0.992	0.854/0.825
	Individual	0.998/0.997	0.970/0.962

VIII. ACKNOWLEDGMENT

Thanks to M. Vrakopoulou for the wind power scenarios.

REFERENCES

[1] D.S. Callaway and I. Hiskens, "Achieving Controllability of Electric Loads," *Proceedings of the IEEE*, 99(1):184-199, 2011.

[2] J.L. Mathieu, M. Gonzalez Vaya, and G. Andersson, "Uncertainty in the flexibility of aggregations of demand response resources," *Proceedings of IECON*, pp. 8052-8057, 2013.

[3] J.L. Mathieu, M. Kamgarpour, J. Lygeros, G. Andersson, and D. Callaway, "Arbitraging intraday wholesale energy market prices with aggregations of thermostatic loads," *IEEE Trans Power Systems*, 30(2): 763-772, 2015.

[4] M. Vrakopoulou, J.L. Mathieu, and G. Andersson, "Stochastic Optimal Power Flow with Uncertain Reserves from Demand Response," *Proceedings of HICSS*, pp. 2353-2362, 2014.

[5] Marco C. Campi, Simone Garatti, Maria Prandini, "The scenario approach for systems and control design," *Annual Reviews in Control*, 33(2): 149-157, 2009.

[6] K. Margellos, P. Goulart, and J. Lygeros, "On the Road Between Robust Optimization and the Scenario Approach for Chance Constrained Optimization Problems," *IEEE Transactions on Automatic Control*, 59(8): 2258-2263, 2014.

[7] D. Bienstock, M. Chertkov, and S. Harnett, "Chance-Constrained Optimal Power Flow: Risk-Aware Network Control under Uncertainty," *SIAM Review*, 56(3): 461-495, 2014.

[8] L. Roald, F. Oldewurtel, T. Krause, and G. Andersson, "Analytical reformulation of security constrained optimal power flow with probabilistic constraints," *Proceedings of PowerTech*, 2013.

[9] M. Vrakopoulou, K. Margellos, J. Lygeros, and G. Andersson, "A Probabilistic Framework for Reserve Scheduling and N-1 Security Assessment of Systems With High Wind Power Penetration," *IEEE Trans Power Systems*, 28(4): 3885-3896, 2013.

[10] R.D. Zimmerman, C.E. Murillo-Sanchez, and R.J. Thomas. "Matpower: Steady-state operations, planning, and analysis tools for power systems research and education." *IEEE Trans Power Systems*, 26(1):12-19, 2011.